MINERALOGICAL MAGAZINE, MARCH 1985, VOL. 49, PP. 37–48

Structural variation in wollastonite and bustamite

R. J. ANGEL

Department of Earth Sciences, University of Cambridge, Downing Street, Cambridge CB2 3EQ

ABSTRACT. The structures of bustamite and the polytypes of wollastonite are shown to be derived from variations in the stacking sequence of a single type of structural unit. This structural unit is a column of unit cells of wollastonite along the *b*-axis and is bounded by (100) and (001) planes ($P\bar{1}$ cell); these units may be stacked together along [100] and [001] with either zero displacement between successive units, or a relative displacement of $\frac{1}{2}$[010]. Regular stacking sequences give rise to the ordered structures of wollastonite polytypes and of bustamite, while the transformations between these structures proceed by the propagation of line defects with Burgers vectors of $\frac{1}{2}$[010] which thus change the stacking sequence of the structural units.

KEYWORDS: crystal structure, wollastonite, bustamite.

SILICATE minerals are commonly classified by the way in which the silicate tetrahedra are linked together (e.g. Zoltai, 1960; Liebau, 1972). More detailed work often subsequently emphasizes structural differences between minerals of the same family, due to the variations in the content of the cation sites within the structure; the stable configuration in each case arises from the interaction between these cation sites and the silicate tetrahedra. Such analysis of structural variation thus depends upon the availability of detailed structure determinations.

A more general approach has been to describe structural families in terms of 'building blocks' of structurally compatible units. The stable structure is then that in which the interactions between the building blocks minimize the internal energy, the interactions in turn being dependent upon the intensive variables imposed on the system. Polytypes are one example of such a system. As strictly defined, all units (layers) are identical in chemical composition and atomic positions, the various polytype structures differing only in the stacking sequence of the layers. However, Thompson (1981) has pointed out that, due to the stacking sequence itself, the layers in a particular polytype need not be crystallographically equivalent, so that the condition of strict structural and chemical equivalence might be relaxed in a practical definition of polytypism. Thompson therefore proposed that the term 'polytypism' should be used to describe the family of structural variants generated by changes to the stacking sequence of structurally compatible units, provided the overall chemistry is unchanged by changes in the stacking sequence. This definition includes, but is not limited to, the classical polytypes such as SiC, graphite, etc., since it also includes such stacking sequences as *AABAAB* . . . and *AABABAAABABA* . . . even when the structural units *A* and *B* are quite distinct. If, however, a structural family arises in which the proportions of distinct structural units changes, e.g. *AAA* . . ., *ABAB* . . ., and *BBB* . . ., the chemistry is varied and such structures are said to form a 'polysomatic series'. Examples of such series include the biopyriboles (biotite–pyroxene–amphibole) which may be described in terms of octahedral and tetrahedral sheets which are in turn comprised of smaller sub-units of structure (Thompson, 1970). The pyroxenoid family of chain-silicate minerals may be regarded in terms of structural units of planar slabs of wollastonite and pyroxene (Koto *et al.*, 1976).

The distinction between polytypes and polysomatic series is important in determining the possible mechanisms of transformation between members of a structural family when one such structure becomes thermodynamically unstable with respect to another owing to a change in the intensive variables. In the case of polysomatic series, the structures may differ not only in the relative displacements of the structural units, but also in the proportions of each type of unit; transformations may therefore require the interconversion of various types of structural unit. In some cases this may be achieved by shear, as in the pyroxenoid minerals (Angel *et al.*, 1984), but more often requires total reconstruction of the structure. By contrast, polytypes which differ only in the relative displacements of one type of structural unit may always be interconverted by introducing a shear between successive structural units.

The polytypic relationship between the structures of wollastonite and parawollastonite was first recognized by Ito (1950). Subsequent studies by both

X-ray diffraction and TEM have demonstrated the existence of a large family of structures related polytypically to triclinic wollastonite, as well as numerous examples of disordered and partially ordered variants. X-ray structure determinations by Trojer (1968) of parawollastonite, and by Henmi *et al.* (1978, 1983) of longer period polytypes, have shown that these structures may be derived by varying the stacking sequence along [100] of layers of triclinic wollastonite. Both detailed structural analysis (Trojer, 1968) and the fact that the measured molar volumes of the polytypes (Wenk, 1969; Henmi *et al.*, 1978, 1983) differ by about 1 %, suggest that the deviations from the ideal structure produced by the simple stacking of layers of triclinic unit cells are very small. That is, wollastonite shows what might be termed 'ideal polytypism'.

Polytypism and disordered polytypic stacking is common in wollastonite. However, despite the structural similarities between the two minerals, no such stacking modifications have previously been observed in bustamite. A survey of a number of synthetic and natural bustamites has therefore been undertaken to ascertain whether polytypes of bustamite, analogous to those of wollastonite, actually exist. The results of this survey by high resolution TEM are presented below, after a detailed review of the structural relationship between wollastonite and bustamite.

Structures. Wollastonite and bustamite are *dreierketten* pyroxenoids, that is they are single-chain silicates with three tetrahedra in each repeat unit along the chain. The structures of wollastonite and bustamite, viewed down the chain direction, are shown in fig. 1. The silicate chains, which run parallel to the *b*-axis in the cell setting used here, are linked together by bands of large cations, the oxygens co-ordinating these cations forming approximately close-packed sheets parallel to (101) of wollastonite. The space group of wollastonite in this cell setting is thus $P\bar{1}$, in contrast to the $C\bar{1}$ cell often employed in structural studies of the pyroxenoid mineral structures; in the $C\bar{1}$ cell the displacement discussed below becomes $\frac{1}{2}[001]$ on $(1\bar{1}0)$. Within the octahedral bands there are several structurally distinct cation sites, and it is the distribution and occupancies of these sites which control the relative stabilities of the possible structural variants, a transformation between the structures results in a changed co-ordination of the cation sites by the tetrahedral chains. In wollastonite there are three types of octahedral sites (fig. 2*a*); $M(3)$ sites form a continuous chain along the centre of each octahedral band, while alternating sequences of $M(1)$ and $M(2)$ sites form the edges of the three site-wide bands. The $M(1)$ and $M(2)$ sites are distinguished by their co-ordination to one of the tetrahedral chains. The $M(2)$ site shares oxygens with two adjacent tetrahedra of one chain, while the adjacent $M(1)$ site shares oxygens with two tetrahedra from the same chain which are separated by a third, offset, tetrahedron. The designation of sites as $M(1)$ and $M(2)$ is thus determined by this co-ordination to one of the adjacent tetrahedral chains, and is independent of the cation occupancy of the octahedral sites. Fig. 2*b* shows that a displacement relative to the octahedral band of this one tetrahedral chain by $\frac{1}{2}[010]$ (i.e. by one half of the repeat distance along the chain) relative to the octahedral band results in the interchange in the designation of the sites along one edge of the octahedral band. That is, sites which were $M(1)$

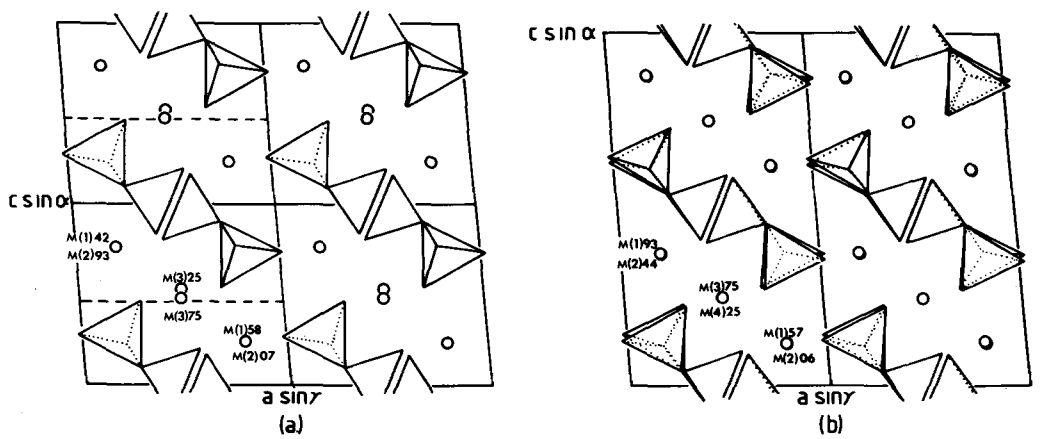

FIG. 1. The structures of wollastonite (*a*) and bustamite (*b*) projected down [010], the chain direction. The structural unit is indicated by the broken lines in (*a*).

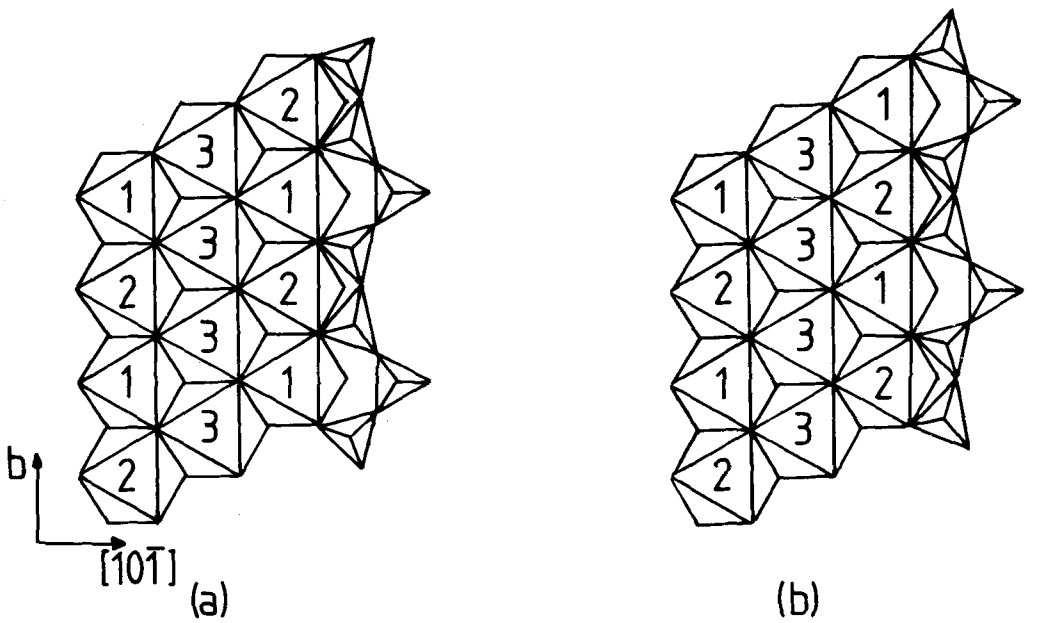

FIG. 2. An octahedral band in wollastonite with one of the adjoining tetrahedral chains, viewed on (101). (*a*) Configuration in $\langle T \rangle$ wollastonite. (*b*) Effect of displacing the tetrahedral chain by $\frac{1}{2}[010]$.

become structurally $M(2)$, while their occupancy remains unchanged. Comparison of figs. 1 and 2 shows that such relative displacements occur when a shear of $\frac{1}{2}[010]$ is introduced on (100); such shears are responsible for the various wollastonite polytypes widely reported in the literature, and these are discussed below.

The bustamite structure may be derived from that of wollastonite by the relative displacement of successive (001) layers of the wollastonite structure by $\frac{1}{2}[010]$, leading to an *A*-face centred cell with a *c* axis double that of wollastonite. The displacement is accompanied by small twistings of the tetrahedra in the silicate chains, but the major change to the structure concerns the octahedral cation sites. In bustamite the $M(1)$ and $M(2)$ sites are co-ordinated in the same way as those in wollastonite, but are distributed differently within each band (compare fig. 2*a* with fig. 6*a*). The relative displacement of the tetrahedral chains across each octahedral band changes the configuration of the chains around the central octahedral sites of the band ($M(3)$ sites in wollastonite) in such a way as to create two sets of non-equivalent sites in bustamite, termed $M(3)$ and $M(4)$. Neither of these has the same environment as the $M(3)$ site of wollastonite.

Following the structure determinations of wollastonite (Mamedov and Belov, 1956; Buerger and Prewitt, 1961) and bustamite (Peacor and Buerger, 1962; Rapoport and Burnham, 1973) further studies have been carried out by Yamanaka *et al.* (1977) and Ohashi and Finger (1978) to determine the relationship between the occupancies of the octahedral sites and their configurations. The composition of wollastonite is commonly restricted to within a few mole % of the ideal composition of $CaSiO_3$, the minor components being Fe, Mn, and Mg, and there is little partitioning between these minor cations and the Ca among the cation sites. By contrast bustamite exhibits strong partitioning of calcium and the other, smaller, cations between the various sites. The Ca-rich limit to bustamite solid solution in the $(Ca,Mn,Fe)SiO_3$ system occurs around 80–5 mol. % $CaSiO_3$ (Abrecht, 1980; Shimazaki and Yamanaka, 1973). This corresponds to all the cation sites in bustamite except $M(3)$ being occupied by Ca (Yamanaka *et al.*, 1977; Ohashi and Finger, 1978). The Ca-poor limit to bustamite on the $CaSiO_3$-$MnSiO_3$ join is around 33 mol % $CaSiO_3$ (Abrecht and Peters, 1980) and corresponds to octahedral site occupancies of $Mn\{M(1), M(3)\}$, $Ca\{M(4)\}$, and $Ca_{0.5}Mn_{0.5}\{M(2)\}$ (Ohashi and Finger, 1978). Between these two limits bustamite undergoes stepwise ordering; with increasing Ca content $M(2)$ and then $M(1)$ are filled by Ca.

A miscibility gap therefore exists between wollastonite and bustamite, and a transformation

mechanism is required that will convert one structure to the other in response to a change in temperature or composition. Such a mechanism must correctly re-arrange the tetrahedral chains and redistribute the cation sites. Takeuchi (1971) proposed a mechanism for this transformation which produces the required displacements of the tetrahedral chains by rotation of individual tetrahedra within the chains and by breaking and reforming some of the Si-O(nbr) bonds. Such a mechanism represents an extrapolation of the trend of increasing tetrahedral rotation with increasing Ca content observed in ferrobustamites by Yamanaka *et al.* (1977). If such a mechanism is applied to the chains in alternate (001) layers of wollastonite the correct bustamite structure is generated. However, the resultant interconversion of $M(1)$ and $M(2)$ sites without concurrent movement of the cations within them will result in some cations residing in structurally unsuited sites. Such a distribution of cations will also be effectively disordered over the new sets of equivalent sites in the structure because, for example, the $M(1)$ sites converted from the $M(2)$ sites in wollastonite will have one population, while those $M(1)$ sites inherited unchanged from the wollastonite will have another. Both of these factors will tend to destabilize the resultant bustamite structure, and may be removed by the transfer of cations along the chains of $M(1)$ and $M(2)$ sites within the bands. The net effect of such a mechanism of tetrahedral chain rotation followed by cation redistribution is identical to that produced by creating the bustamite structure from wollastonite by a $\frac{1}{2}[010]$ shear on (001). Whether the true mechanism is that of Takeuchi, or one of simple shear, we can model the structural change purely in terms of the displacement of (001) layers of the structure; we would then expect to find intergrowths of wollastonite and bustamite on (001), and disordered stacking sequences along [001] due to random sequences of displacements of successive (001) layers.

The two types of shear mechanisms invoked to derive both the wollastonite polytypes and bustamite from triclinic wollastonite employ a shear of $\frac{1}{2}[010]$, but on different planes. Taken together they define a structural unit which may be used to generate both types of structural variation. This unit is an infinite column of unit cells of wollastonite extending along [010], the chain extension direction, and limited in cross-section to a single wollastonite cell bounded by (100) and (001) planes (fig. 1*a*). Each successive unit along [100] and [001] may be displaced by $\frac{1}{2}[010]$ relative to the preceding unit, or may remain undisplaced. The wollastonite polytypes arise through the variation of the stacking along [100] alone, with no displacements in the sequence along [001]. Similarly wollastonite–bustamite stacking variations will result from variations in the stacking sequence along [001] alone. Finally, other structures may be derived by allowing variation along both axes. It is therefore apparent that if the proposed structural unit is employed, the classical wollastonite polytypes, together with bustamite, provide an example of two-dimensional polytypism. Fig. 3 illustrates some of the possible structures which may be generated by variations in the stacking of the structural units along the [100] axis in both bustamite and wollastonite. The diagrams are in approximately the same orientation as those of fig. 1, the (010) plane being parallel to the paper with the prismatic structural units being viewed approximately end on. Within each grid square, each of which represents one structural unit, an open circle represents a unit undisplaced along [010] relative to some arbitrary origin, and a closed circle represents a unit displaced by $\frac{1}{2}[010]$. The basic wollastonite structure is seen to be comprised of undisplaced structural units, whereas the corresponding bustamite polytype has each successive (001) layer of structural units displaced by $\frac{1}{2}[010]$. Fig. 3*a*, *d* should be compared with fig. 1.

The *T*,*G* notation employed in fig. 3 was introduced by Henmi *et al.* (1978) to describe stacking sequences in the polytypes of wollastonite, but is equally applicable to any structure in the wollastonite–bustamite family, such as bustamite itself, which has a regular stacking sequence along [001]. The notation describes the sequence of translation operators required to generate the stacking sequence along [100] of identical (100) layers of structural units. Each successive layer may be undisplaced along [010] relative to the previous one, denoted *T* in the notation due to Henmi *et al.* (1978), or may be displaced by $\frac{1}{2}[010]$, this being denoted *G*. Any regular stacking sequence is then written as the repeat unit alone, and bracketed. Thus the regular sequence *TTGGTTGG* . . . is written $\langle TTGG \rangle$. If the layers are all stacked without relative displacement, that is $\langle T \rangle$, the basic one-layer polytype is generated (denoted $1T$ by earlier workers). It should be noted that, due to the pseudo-monoclinic symmetry of the structural unit, a stacking sequence $\langle G \rangle$ also generates this same structure, but in a twin orientation to that of $\langle T \rangle$ (Hutchison and McLaren, 1977). The other polytypes arise from other regular sequences of stacking vectors. For example parawollastonite, the monoclinic polytype, has the stacking formula $\langle TG \rangle$, a three-layer polytype found by Henmi *et al.* (1983) has the formula $\langle TTG \rangle$. The $\langle T \rangle$,$\langle G \rangle$, and $\langle TG \rangle$ structures of both wollastonite and bustamite are illustrated in fig. 3.

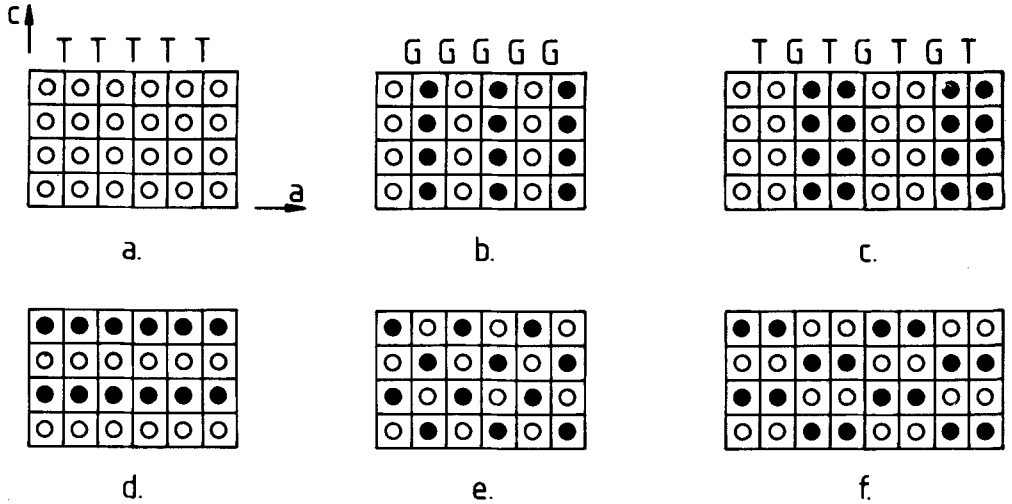

FIG. 3. Structural unit stacking configurations viewed on (010). Open symbols represent undisplaced units, filled symbols units displaced by $\frac{1}{2}$[010]. (*a*) $\langle T \rangle$, (*b*) $\langle G \rangle$, (*c*) $\langle TG \rangle$ polytypes of wollastonite. (*d*) $\langle T \rangle$, (*e*) $\langle G \rangle$, (*f*) $\langle TG \rangle$ polytypes of bustamite.

Polytypism in bustamite

A number of synthetic and natural bustamites were examined for polytypic stacking variation on (100). The method of characterization was by high resolution TEM, as this allows a direct determination of the stacking sequence in suitably oriented specimens, whereas considerable problems arise in the analysis of disordered, and partially ordered, stacking sequences by X-ray diffraction (Jefferson, 1972). All the experimental images were taken with a JEOL JEM-100CX electron microscope operating at 100 kV, with an objective aperture to limit the number of diffracted beams contributing to the image. These images were matched to computer simulations produced by the program SHRLI (O'Keefe and Buseck, 1979). In the case of those images taken with the smaller objective aperture of effective radius 0.2 $Å^{-1}$, the white spots observed correspond to areas in the structure of low projected electrostatic potential, and each spot may be associated with a single unit cell of the structure.

Observations. The natural bustamites examined for evidence of polytypism were from a range of environments, and spanned a range in composition from near to the limit of minimum Ca content (samples from Treburland, Cornwall), to high Ca bustamites (compositions around Ca : Mn + Fe = 0.79 : 0.21) from Broken Hill, Australia. Observations were also made on several Fe-containing bustamites from contact skarns which were described by Tilley (1937, 1947) as 'iron-wollastonite solid solutions'. None of these samples showed any evidence of polytypic stacking variation, the only faults on the (100) plane being occasional macroscopic twins. These twins, as in wollastonite, are due to a change in stacking formula from $\langle T \rangle$ to $\langle G \rangle$, but this twinning does not appear to occur on a unit cell scale to give rise to stacking disorder in natural bustamites, as it does in wollastonite.

Synthetic bustamites were produced in two ways. Natural johannsenite, a Ca–Mn clinopyroxene, was heated in an atmosphere of argon at 900 °C to invert it to bustamite. Multiple twins on a unit cell scale were observed in this bustamite, but no regular stacking sequences were observed which could be identified as polytypes of bustamite (fig. 4). Bustamites were also made by the devitrification of a chemically homogeneous glass of composition close to $Ca_{0.5}Mn_{0.5}SiO_3$. In these bustamites, as in those inverted from clinopyroxene, evidence was found of polytypic stacking disorder, notably in those samples which were subjected to shorter annealing times. Fig. 5*a* is a micrograph of such a region, oriented with [001] parallel to the electron beam. The micrograph shows planar faults parallel to (100) with displacements of $\frac{1}{2}$[010] occurring at random intervals within the structure. The associated diffraction pattern (fig. 5*b*) shows intense spots on $k = 2n$ rows, corresponding to maxima from the normal bustamite structure. Associated with these spots is weak streaking which may either be caused by small deviations of the stacking vector from the ideal $\frac{1}{2}$[010] (Jefferson, 1972) or by dy-

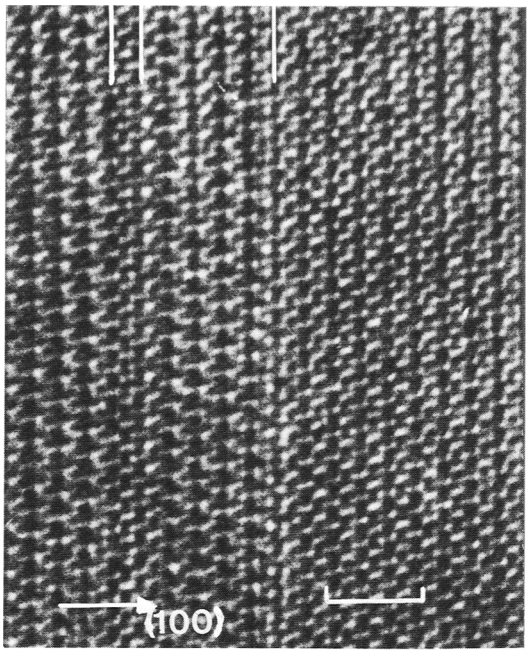

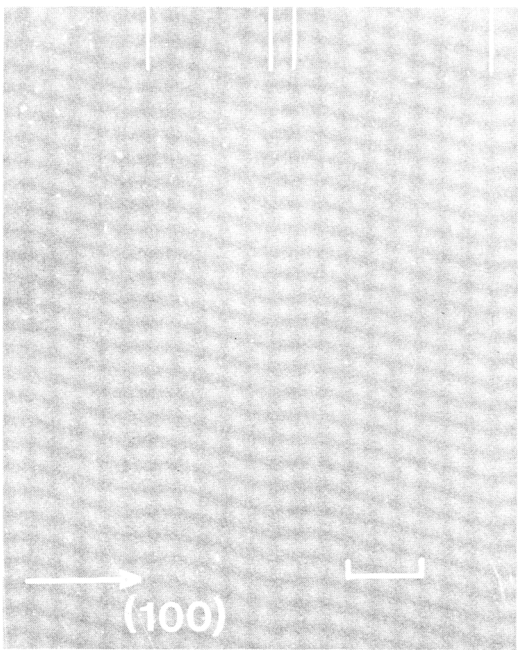

FIG. 4. High-resolution micrograph of (100) twinning in bustamite, with the electron beam parallel to [0$\bar{1}$1], the twin boundaries are marked. Scale bar is 30 Å, objective aperture radius was 0.33 Å^{-1}.

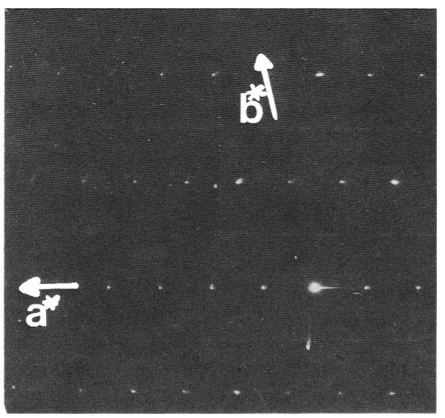

FIG. 5. (*a, top*) High resolution micrograph of stacking disorder on (100) in bustamite viewed down [001], the (100) faults being indicated. Scale bar is 30 Å, objective aperture was 0.20 Å^{-1}. (*b, bottom*) Associated selected area diffraction pattern.

namical diffraction effects as suggested by Muller (1976) in his TEM study of the polytypism of the structurally similar minerals pectolite and serandite. On the $k = 2n+1$ rows, which would not normally be present due to the *A*-lattice of bustamite, there are streaks parallel to a^* which show a number of minor maxima. This indicates that the structure has lost its *A*-lattice and is now primitive. This may arise in several ways; it may be that the sections showing this disorder are in fact wollastonite, but this seems unlikely in a sample formed from a chemically homogeneous glass at a composition so far from the wollastonite stability field. Furthermore, the maxima on the $k = 2n+1$ rows do not appear at positions expected from the shorter period wollastonite polytypes. Alternatively the sections may contain sufficient wollastonite–bustamite stacking faults on (001) to violate the *A*-lattice and promote polytypism. In view of the difficulty in producing these inversion faults even within the miscibility gap between the two structures, this too seems improbable, and no inversion faults were observed in [100] sections of these samples. The conclusion must therefore be that distortions associated with the $\frac{1}{2}[010]$ displacement used to create the polytypic stacking disorder reduce the symmetry of the structure from $A\bar{1}$ to $P\bar{1}$.

Discussion. The TEM observations reported above suggest that, in contrast with wollastonite, polytypes of bustamite are thermodynamically unstable with respect to the common $\langle T \rangle$ structure. A study of these faults, and comparisons between the wollastonite and bustamite structures, enable the relative stability of wollastonite poly-

types and instability of bustamite polytypes to be explained.

The polytypes of wollastonite may be transformed from one to another by the introduction of shears of $\frac{1}{2}[010]$ on (100). As described above, the introduction of such shears on some (100) planes will convert the $M(1)$ sites adjacent to the shear planes into $M(2)$ sites, and vice-versa. If such shears are introduced periodically into the $1T$ wollastonite structure, $\langle T \rangle$, an ordered stacking sequence of longer period is generated in which the formerly $M(1)$ sites of the $\langle T \rangle$ structure which were adjacent to the shear planes are now structurally equivalent to the $M(2)$ sites in the remainder of the structure, and vice versa. This is illustrated by the structure of monoclinic parawollastonite which was refined by Trojer (1968); this example also enables us to distinguish between the Takeuchi model of tetrahedral chain movement, and the shear model for generating polytypes.

Parawollastonite, often designated $2M$ wollastonite, has the stacking formula $\langle TG \rangle$ and may thus be derived from the $\langle T \rangle$ structure by the introduction of $\frac{1}{2}[010]$ shears after every alternate cell along [100]. Consider the $M(1)$ sites of two unit cells of triclinic wollastonite (fig. 1*a*), these two cells then being bounded by shears on (100). The two $M(1)$ sites in the interior of the block of two cells remain unchanged in co-ordination but, as described above, the two $M(2)$ sites adjacent to the shear planes are converted to equivalents of $M(1)$, but remain undisplaced in position. Comparison of this structure generated by shears from $\langle T \rangle$ wollastonite with the structure of parawollastonite shows that this model correctly reproduces the distribution of equivalent cation sites required by the space group of parawollastonite, $P2_1/m$. Although the mechanism of tetrahedral chain movement proposed by Takeuchi (1971) also generates this distribution of sites within one unit cell of parawollastonite, the sites in the next unit cell are displaced by $\frac{1}{2}[010]$ from their correct positions. We may therefore conclude that entire structural units, rather than the tetrahedral chains alone, must be displaced in order to effect these transformations between polytypes.

By simple comparison we might expect a $\langle TG \rangle$ 'parabustamite' structure to exist which would be the *A*-lattice analogue of parawollastonite. However, as described above, the transition from $\langle T \rangle$ to $\langle TG \rangle$ changes the structure of the cation sites adjacent to the shear planes, but leaves the occupancy of these sites unchanged. In wollastonite this is not critical, as structure refinements (Ohashi and Finger, 1978) indicate that there is very little partitioning of cations between $M(1)$ and $M(2)$, whereas considerable partitioning of Ca and other cations does occur between these two sites in bustamite. Generation of the $\langle TG \rangle$ polytype of bustamite by shear alone would thus lead to some $M(1)$ type sites being Ca rich, and some $M(2)$ sites being Ca poor. This is illustrated in fig. 6 for the

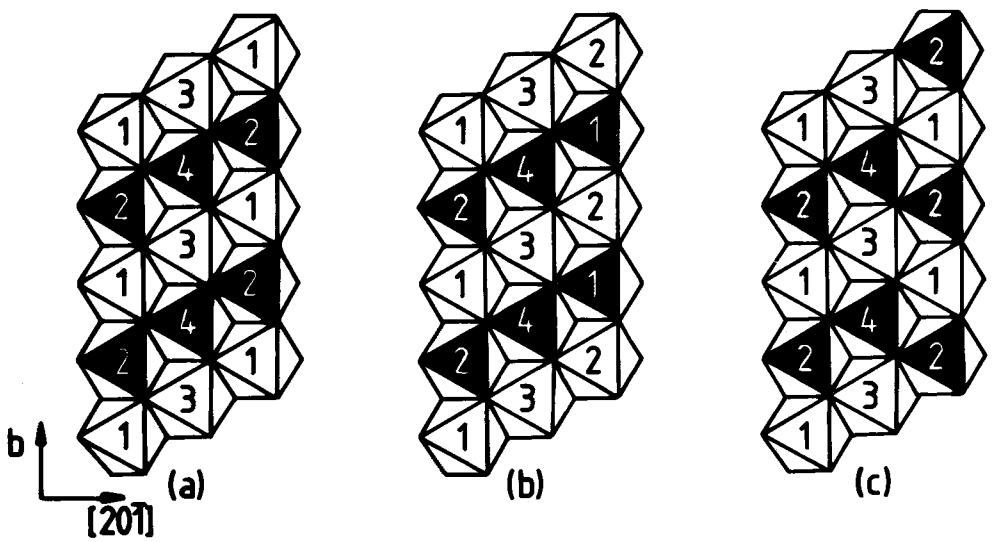

FIG. 6. (*a*) An octahedral band in a bustamite of composition $CaMnSi_2O_6$ viewed on (102). (*b*) The same band after displacement of the adjacent tetrahedral chain, and (*c*) after redistribution of the cations. Shaded octahedra are occupied by Ca.

$Ca_{0.5}Mn_{0.5}SiO_3$ composition. If this distribution of cations is retained, then not only are the sites adjacent to the shear plane occupied by the wrong cations, but Ca-rich and Ca-poor sites are now related by the symmetry of the $\langle TG \rangle$ structure, effectively disordering these cations over the new sets of equivalent sites in the structure. Both of these factors will destabilize the structure. Alternatively, the cations adjacent to the shear planes may be returned to structurally more suitable sites, as in fig. 6*c*. Although this configuration would be stabilized by the correct matching of occupancies and site configurations, this distribution of cations within the octahedral bands has not been observed before. Its instability may be related to the change in distribution of octahedral edges shared with Ca-rich sites by the $M(3)$ site, which appear to force this small Mn site to expand.

Trojer (1968) also noted that the minor shifts in atomic co-ordinates in parawollastonite from the ideal positions generated from shearing the $\langle T \rangle$ structure result in the loss of some of the centres of symmetry inherited from the $\langle T \rangle$ structure. Such shifts are obviously due to the structure minimizing the internal energy due to strain, the loss of centres of symmetry being an indicator of this process. Bustamite, however, possesses a different distribution of centres; in particular the $M(3)$ and $M(4)$ sites lie on centres, whereas in wollastonite these sites are equivalent $[M(3)]$ and are related by the centres. We may therefore suggest that the relaxation to remove the internal strain in bustamite polytypes is not necessarily able to follow that of wollastonite, but instead results in the loss of the *A*-face centring as indicated by the diffraction patterns (fig. 5*b*).

Polytype instability in bustamite is thus due to the cation partitioning between $M(1)$ and $M(2)$ of the $\langle T \rangle$ structure, although this would be minimized at Ca-rich compositions when both sites have similar high Ca contents, and possibly due to different constraints imposed upon the relaxation of a $\langle TG \rangle$ structure by the $M(3)$ and $M(4)$ cation sites from those due to the $M(3)$ site of wollastonite.

Wollastonite-bustamite inversion

The inversion between bustamite and wollastonite involves changes to the stacking sequence of the structural units along [001], in contrast to wollastonite polytypism which is due to varied stacking sequences along [100] of (100) layers of wollastonite structure; in that case the layers are comprised of structural units with no relative displacement between them along [001]. The inversion of wollastonite to bustamite, or the formation of intergrowths of the two structures is more complex than polytypism in wollastonite in that the intergrowths may be between bustamite and any one of the wollastonite polytypes. Akai (1975), in a study of natural wollastonites, reported b^*-c^* diffraction patterns of $\langle T \rangle$ wollastonite which show faint streaking parallel to c^* on k-odd rows. These he correctly attributed to faults on (001) which have an associated displacement of $\frac{1}{2}[010]$. In view of the discussion given here, we can now interpret these faults as giving rise to small portions of bustamite structure within a matrix of $\langle T \rangle$ wollastonite. No intergrowths involving bustamite polytypes have been reported in the literature, or observed during the current work.

Observations. The inversion of the $\langle TG \rangle$ polytype of wollastonite to bustamite has been observed in synthetic material produced by annealing a glass of composition $Ca_{0.81}Mn_{0.22}Si_{0.98}O_3$ at 1200 °C which resulted in a mixture of the $\langle T \rangle$ and $\langle TG \rangle$ polytypes of wollastonite. This material was then reheated in the miscibility gap between wollastonite and bustamite at 785 °C for $6\frac{1}{2}$ days, and then quenched. Examination of crushed grains of this sample by high resolution TEM showed that much of the sample had remained as wollastonite, and showed no evidence of inversion to bustamite. However, intergrowths of wollastonite and bustamite were observed in some sections of $\langle TG \rangle$ wollastonite when viewed with the electron beam parallel to the [100] zone axis of the *monoclinic* unit cell of the $\langle TG \rangle$ wollastonite (fig. 7*a*). The associated diffraction pattern (fig. 7*b*) clearly identifies the matrix as the $\langle TG \rangle$ polytype of wollastonite by the characteristic pattern of low intensities of diffracted beams with $k = 4n+2$ (n integer) as noted by Trojer (1968). The bustamite and wollastonite share (001) as the composition plane as predicted by the inversion mechanism, and therefore the orientation of the bustamite in the micrograph of fig. 7 is such that the electron beam is parallel to [410] of bustamite, so that the bustamite lamellae only contribute diffracted intensity to the maxima of the diffraction pattern with $k = 4n$. The streaking parallel to c^* on k odd rows of the diffraction pattern cannot therefore be due to the change in stacking sequence along [001] on moving from wollastonite to bustamite, but is a result of the wollastonite matrix containing several bustamite lamellae of different widths. Because the compositions of these lamellae presumably differ from that of the matrix, the lattice parameters of the bustamite will not be exact multiples of those of wollastonite. Consequently areas of wollastonite matrix separated by a lamella will be displaced from their ideal, in-register, position by an amount dependent on the lamella width, thus giving rise to streaking.

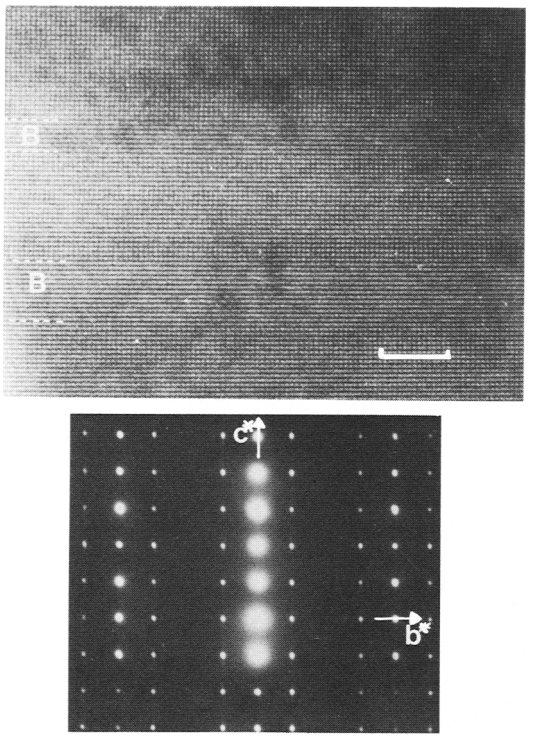

FIG. 7. (*a, top*) High-resolution micrograph of exsolution of (001) bustamite lamellae (B) from ⟨*TG*⟩ wollastonite. Scale bar is 100 Å, objective aperture was 0.20 $Å^{-1}$. (*b, bottom*) The associated selected area diffraction pattern.

⟨*TG*⟩, rather than the ⟨*T*⟩ polytype of wollastonite, and appear to have nucleated on (100) faults within ⟨*T*⟩ wollastonite. The intergrowth could therefore be an area of wollastonite partially inverted to bustamite, the inversion being driven by an increase in iron content, or it could be the result of the simultaneous growth of wollastonite and bustamite. The lamellae of ⟨*TG*⟩ wollastonite within the matrix of bustamite (fig. 8) show the same orientational relationship as the synthetically produced material, the (001) plane being common to both phases.

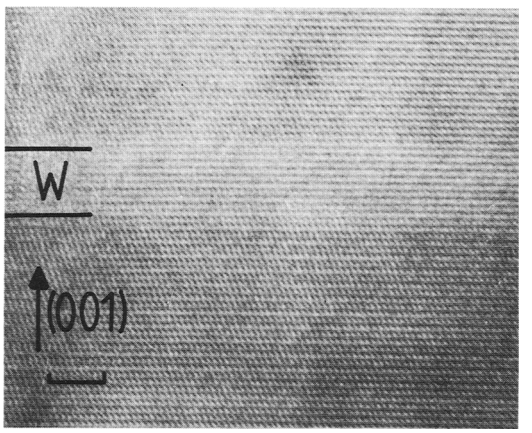

FIG. 8. High-resolution micrograph of a ⟨*TG*⟩ wollastonite lamella (W) within a matrix of bustamite. Scale bar is 30 Å, objective aperture was 0.20 $Å^{-1}$.

Similar intergrowths of bustamite with wollastonite have been observed in natural material first described by Tilley and Harwood (1931) as 'zoned iron-wollastonite' from the endogeneous contact zone of a dolerite dyke in chalk at Scawt Hill, County Antrim, Northern Ireland. Further details of this 'iron-wollastonite' were described in a subsequent paper by Tilley (1937), and the material was analysed by Shimazaki and Yamanaka (1973), who concluded that the cores of the grains were wollastonite, and that the rims were Fe-rich bustamite. High resolution TEM has been carried out on suitably oriented zoned crystals removed from petrographic thin section and thinned by ion-milling. Electron diffraction patterns confirmed the identification of the cores of these grains as wollastonite, mainly of the ⟨*T*⟩ polytype but with some areas of the ⟨*TG*⟩ polytype and of highly disordered stacking. The rims of the grains are well crystallized bustamite almost totally devoid of faults. As in the synthetic material described above, the intergrowths are between bustamite and the

Discussion. It has been shown that inversion from wollastonite to bustamite will occur as a response to a suitable change in composition, such as increasing the iron content as in the Scawt Hill samples, or to a change in temperature. However, the experiments with synthetic material on the join $CaSiO_3$–$MnSiO_3$ do indicate that wollastonites with compositions above the miscibility gap may be quenched through the gap without inversion, and that considerable annealing times may be required to produce inversion in the absence of a fluid phase.

The fact that inversion from the ⟨*TG*⟩ polytype of wollastonite has been observed indicates that structural variation between wollastonite and bustamite is not due to variations in the stacking sequence of (001) sheets of wollastonite alone. The inversion from the ⟨*T*⟩ polytype of wollastonite to bustamite can be described in these terms, since the wollastonite and the bustamite have the same stacking sequence along [100] (fig. 3). In this case the (001) sheets of structural units are undisplaced

in the wollastonite matrix, and the introduction of a $\frac{1}{2}[010]$ displacement between each successive sheet will generate lamellae of bustamite. But in the case of the inversion from the $\langle TG \rangle$ polytype of wollastonite the stacking sequence along [100] in the matrix differs from that in the bustamite lamellae. Consequently the displacement of (001) layers of the $\langle TG \rangle$ wollastonite in a manner analogous to that used for the $\langle T \rangle$ polytype would generate a $\langle TG \rangle$ polytype of bustamite rather than the correct $\langle T \rangle$ structure. Consideration of the configuration of the structural units in bustamite and the $\langle TG \rangle$ polytype of wollastonite (fig. 3) shows that the displacement of isolated pairs of structural units within the $\langle TG \rangle$ structure will generate the correct bustamite structure. Since bustamite type faults, or inversion, have been observed in two wollastonite polytypes it seems reasonable to suppose that inversion is possible from any wollastonite polytype. All inversions, except that from the $\langle T \rangle$ polytype, must involve the displacement of either individual structural units or groups of such units if the stable $\langle T \rangle$ polytype of bustamite is to be produced.

Transformations

Since all of the members of the wollastonite–bustamite structural family may be described in terms of the stacking of a single structural unit, transformations from one structure to another may be achieved by changing the relative displacements of the structural units. Observations made on bustamite produced by the inversion of johannsenite (a clinopyroxene) suggest how this may occur. The initial product on annealing the clinopyroxene in the bustamite stability field is a bustamite showing twinning on (100) on a fine scale (fig. 4), while further annealing produces well-crystallized bustamite devoid of such faults. The annealing process, on a structural unit scale, must therefore change a stacking sequence along [100] consisting of a mixture of $\langle T \rangle$ and $\langle G \rangle$ sequences of varying length into a continuous sequence of

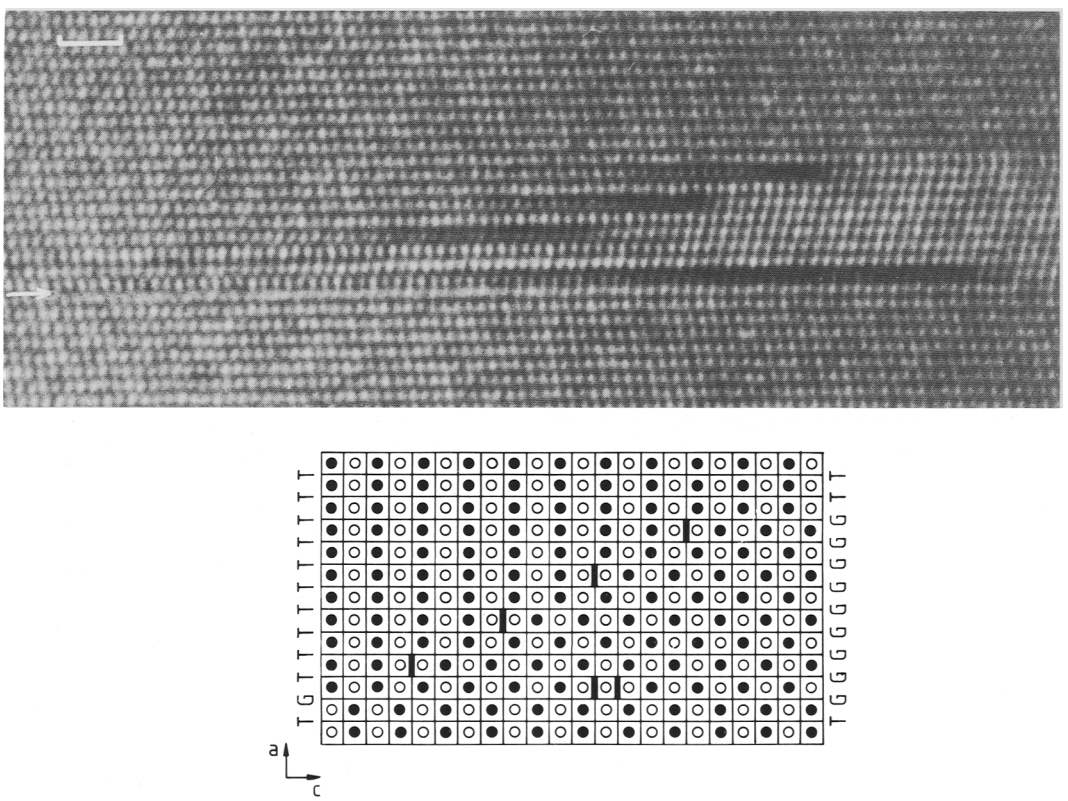

FIG. 9. (*a*, *top*) High-resolution micrograph of a (100) twin lamella being removed from bustamite by the propagation of $\frac{1}{2}[010]$ line defects, viewed down $[0\bar{1}1]$. The residual *G* fault is arrowed, the scale bar is 30 Å, the objective aperture was 0.20 $Å^{-1}$. (*b*, *bottom*) The interpretation of this area in terms of structural units viewed down [010].

$\langle T \rangle$ or $\langle G \rangle$. Fig. 9*a* is a micrograph of one such region of bustamite in the process of eliminating a short sequence of $\langle G \rangle$ stacking which forms a (100) twin lamella, from a matrix of $\langle T \rangle$.

The orientation of the specimen is such that the electron beam is parallel to $[0\bar{1}1]$, so that the *b*-axis of the structure is thus inclined to the plane of the specimen by about 37 deg. Care is therefore necessary in interpreting the micrograph in terms of structural units being displaced parallel to the *b*-axis, but the comparison of stacking sequences at the two extremes of the micrograph allows the nature of the faults to be deduced. The stacking sequence of structural units which would reproduce the structure seen in fig. 9*a* is presented in fig. 9*b*. It can be seen that some of the (100) layers of bustamite structure contain line defects running parallel to [010], across which adjacent units are undisplaced and thus form small volumes of wollastonite-type structure. When these faults are viewed at an inclined angle in the electron microscope, as in fig. 9*a*, these faults appear as dark bands which lie parallel to the (100) fringes of the bustamite. Consideration of fig. 9*b* shows that if these line defects have an associated Burgers vector of $\frac{1}{2}[010]$, and if propagated through the structure along [001], they will convert the $\langle G \rangle$ stacking sequence of the twin lamella into the $\langle T \rangle$ sequence of the matrix. Thus the lamella would be removed, except that in this case the lamella contained an odd number of *G* stacking operators, and thus the $\langle T \rangle$ matrix will still contain a residual *G* operator after the removal of the lamella. This residual fault can be seen at the left hand end of fig. 9. Lamellae containing an even number of *G* operators may be completely eliminated from a matrix of $\langle T \rangle$ since the total displacement across the lamella due to the stacking operators will be an integral number of unit cells.

Transformations between members of the wollastonite–bustamite structural family thus proceed by the propagation through a structure of line defects running parallel to the *b*-axis. The example given above shows that the stacking sequence of (100) structural units may be changed by the propagation of these line defects along [001]. Similarly, a change in the stacking sequence of (001) layers of structural units, as in the case of $\langle T \rangle$ wollastonite transforming to $\langle T \rangle$ bustamite, may be carried out by the propagation along [100] of similar defects. Transformations between other pairs of stacking sequences may proceed by the movement of the same line defects on other (*h*0*l*) planes. It is interesting to note that a $\langle T \rangle$ wollastonite structure may be transformed to a $\langle T \rangle$ bustamite structure as described above, while propagation of the defects along the (101) planes of the wollastonite would generate a bustamite with stacking sequence $\langle G \rangle$.

Conclusions

Careful consideration of the structures of the wollastonite polytypes and bustamite has shown that they may all be derived from variations in the stacking sequence along two axes, [100] and [001], of a prismatic structural unit consisting of a stack of unit cells of $\langle T \rangle$ wollastonite along [010]. These structures therefore form a polytypic family in the sense of Thompson (1981), but one in which the polytypic variation is two dimensional rather than being restricted to one dimension as is the case in classical polytypic systems. The observation by high-resolution electron microscopy of the inversion of $\langle TG \rangle$ wollastonite to bustamite also provides evidence for the reality of these structural units. This inversion requires the displacement of individual pairs of structural units, as opposed to the sheets of structure displaced in either the transformations between polytypes, or the inversion from $\langle T \rangle$ wollastonite to bustamite. The description of the structures in terms of structural units which possess the same essential structural features also means that transformations between two regular stacking sequences may proceed by the relative displacement of the structural units without any major change to the internal structure of the units. The observations presented here suggest that these displacements are introduced into a structure by the propagation through the structure of line defects parallel to the *b*-axis, with an associated Burgers vector of $\frac{1}{2}[010]$. Relatively minor changes, such as small rotations of the silicate tetrahedra and local redistribution of the octahedral cations, may occur as a 'relaxation phase' following the movements of structural units.

Acknowledgements. I would like to thank Professor T. G. Vallance of the Geology Department of the University of Sydney for the samples from Broken Hill, and Dr G. A. Chinner, curator of the Harker collection, for the remainder of the specimens used in this study. Thanks are due to Dr G. D. Price of University College, London, and to Dr A. Putnis for valuable guidance and discussions during the period of this work, and to Dr M. G. Bown and Dr A. Putnis for critically reading the manuscript, and a detailed review by Dr J. E. Chisholm of the British Museum was of great help in producing the final version of this paper. I acknowledge the receipt of a NERC research studentship.

REFERENCES

Abrecht, J. (1980) *Contrib. Mineral. Petrol.* **74**, 253–60.
—— and Peters, Tj. (1980) Ibid. **74**, 261–9.
Akai, J. (1975) *Mem. Faculty Sci. Kyoto University*, Series of Geology and Mineralogy **41**(2), 1–14.

Angel, R. J., Price, G. D., and Putnis, A. (1984) *Phys. Chem. Mineral.* **10,** 236–43.
Buerger, M. J., and Prewitt, C. T. (1961) *Proc. Nat. Acad. Sci.* **47,** 1884–8.
Henmi, C., Kawahara, A., Henmi, K., Kusachi, I., and Takeuchi, Y. (1983) *Am. Mineral.* **68,** 156–63.
——Kusachi, I., Kawahara, A., and Henmi, K. (1978) *Mineral J.* **9,** 169–81.
Hutchison, J. L., and McLaren, A. C. (1977) *Contrib. Mineral. Petrol.* **61,** 11–13.
Ito, T. (1950) *Maruzen,* Tokyo. 93–110.
Jefferson, D. A. (1972) *A study of stacking disorder in some silicate minerals.* Ph.D. thesis, Univ. Cambridge.
Koto, K., Morimoto, N., and Narita, H. (1976) *J. Jap. Ass. Mineral. Petrol. Econ. Geol.* **71,** 248–54.
Liebau, F. (1972) In *Handbook of Geochemistry* II/2 (K. H. Wedepohl, ed.). Springer-Verlag, Berlin.
Mamedov, Kh. S., and Belov, N. V. (1956) *Dokl. Acad. Nauk SSSR* **107,** 463–6.
Muller, W. F. (1976) *Z. Kristallogr.* **144,** 401–8.
Ohashi, Y., and Finger, L. W. (1978) *Am. Mineral.* **63,** 274–88.
O'Keefe, M. A., and Buseck, P. (1979) *Trans. Am. Crystallogr. Ass.* **15,** 27–46.
Peacor, D. R., and Buerger, M. J. (1962) *Z. Kristallogr.* **117,** 331–43.
Rapoport, P. A., and Burnham, C. W. (1973) Ibid. **138,** 419–38.
Shimazaki, H., and Yamanaka, T. (1973) *Geochem. J.* **7,** 67–79.
Takeuchi, Y. (1971) *J. Mineral. Soc. Japan* **10,** Special paper 2, 87–99.
Thompson, J. B. (1970) *Am. Mineral.* **55,** 292–3.
——(1981) In *Structure and Bonding in Crystals II* (M. O'Keefe and A. Navrotsky, eds.). Academic Press.
Tilley, C. E. (1937) *Mineral. Mag.* **24,** 569–72.
——(1947) *Bull. Comm. Geol. Finlande* **140,** 97–105.
——and Harwood, H. F. (1931) *Mineral Mag.* **22,** 439–68.
Trojer, F. J. (1968) *Z. Kristallogr.* **127,** 291–308.
Wenk, H.-R. (1969) *Contrib. Mineral. Petrol.* **22,** 238–47.
Yamanaka, T., Sadanaga, R., and Takeuchi, Y. (1977) *Am. Mineral.* **62,** 1216–24.
Zoltai, T. (1960) *Am. Mineral.* **45,** 960–73.

[*Manuscript received 25 July 1984; revised 3 September 1984*]